IAEA nuclear fusion

PAPER • OPEN ACCESS

Comparison of plasma start-up with high Z and low Z first wall in WEST

To cite this article: C. Guillemaut *et al* 2025 *Nucl. Fusion* **65** 036007

OPEN ACCESS
IOP Publishing | International Atomic Energy Agency | Nuclear Fusion

Nucl. Fusion **65** (2025) 036007 (10pp) https://doi.org/10.1088/1741-4326/adaecf

Comparison of plasma start-up with high Z and low Z first wall in WEST

C. Guillemaut[1,*], K. Afonin[1], G. Bodner[2,3], J. Bucalossi[1], Y. Corre[1], P. Devynck[1], A. Diallo[2], M. Diez[1], N. Fedorczak[1], A. Gallo[1], B. Guillermin[1], V. Lapleigne[1], R. Lunsford[2], P. Maget[1], J. Morales[1], Ph. Moreau[1], the WEST Team[a] and the EUROfusion Tokamak Exploitation Team[b]

[1] CEA, IRFM, F-13108 Saint-Paul-Lez-Durance, France
[2] Princeton Plasma Physics Laboratory, Princeton, NJ, United States of America
[3] General Atomics, San Diego, CA, United States of America

E-mail: christophe.guillemaut@cea.fr

Received 3 October 2024, revised 8 January 2025
Accepted for publication 27 January 2025
Published 10 February 2025

Abstract

The choice of first wall material is of paramount importance for the plasma start-up conditions in ITER and future fusion power plants. In this context, the present work focuses on the correlations between first wall impurity sources and total radiated power during plasma start-up in the tungsten (W) Environment in Steady-state Tokamak (WEST). The objective is to highlight experimental indications for a preferable combination of start-up plasma scenario and first wall materials. Until 2019, WEST featured a full high Z first wall with all limiters exposing only W surfaces to the plasma. To study the impact of a low Z first wall in WEST, boron nitride tiles were installed in the central part of the inner and outer limiters in 2020. Although visible spectroscopy and bolometry measurements show respectively a strong weakening of the WI line intensity on the limiters and a reduction of radiated power after the changeover, a degradation occurs with the accumulation of plasma exposure. In addition, the different plasma facing elements of the main chamber do not influence equally the radiated power during start-up. In both high Z and low Z environments, a clear non-linear dependence is found between the start-up radiated power and the outer limiter W impurity source. Since W seems to be the main cause for core radiation, correlation between outer limiter W sources and other impurity sources are investigated. Finally, analysis of the legacy of B powder drops on a number of start-up plasmas suggests that it is less effective at reducing radiated power when the first wall is covered with W.

Keywords: nuclear fusion, plasma surface interaction, visible spectroscopy, plasma start-up, boron, nitrogen, tungsten

Some figures may appear in colour only in the online journal

[a] See http://irfm.cea.fr/en/west/WESTteam/.
[b] See Joffrin *et al* 2024 (https://doi.org/10.1088/1741-4326/ad2be4) for the EUROfusion Tokamak Exploitation Team.
[*] Author to whom any correspondence should be addressed.

1. Introduction

The tungsten (W) Environment in Steady-state Tokamak (WEST) [1, 2] based at CEA Cadarache is an actively cooled superconducting machine presently testing the ITER-like divertor plasma facing units [3]. It featured a full W environment with W coatings [4] on the limiters, the upper divertor and most of the lower divertor until the 2019 experimental campaign. For the 2020 campaign, boron nitride (BN) tiles were installed [5] in the central part of the Inner Bumpers (IB) and the retractable outer Antenna Protection Limiter (APL), see figure 1. Bulk W tiles will replace them at the end of 2024.

The present study is focused on the plasma start-up, namely the dynamic phase just after breakdown and at the beginning of the current ramp. At this moment, the plasma shape is close to circular with no vertical elongation and no contact with the divertor. Due to the position of the IB and the APL, the start-up plasma width cannot be larger than ∼1 m. Since the amplitude of the plasma center movement is typically lower than ±5 cm, it does not allow contact with other objects than the IB and the APL during this phase, see figure 1. With W tiles on these first wall elements, the plasma start-up was often affected by MHD instabilities detrimental for the subsequent divertor phase. Experimental evidences supported by modelling relate high levels of core plasma radiation to a high W content in WEST [6]. During start-up, W must originate from first wall sources.

Early injection of nitrogen (N) in this phase tried during the 2019 campaign helped reducing the W sources by radiative cooling of the scrape-off layer (SOL) and improved notably the plasma conditions with higher core temperature and lower core radiation [7]. In addition, since the 2019 campaign, boronizations are regularly performed to cover the W sources. In 2020, the BN tiles were installed on the IB and the APL to study the impact of a low Z first wall on plasma conditions. In the same campaign and in the 2023 campaign, B powder drops [8–10] were also tested.

An extensive study comparing series of post-boronization start-up discharges in 2019, 2020 and 2023 campaigns using bolometry and visible spectroscopy measurements (see section 2) is presented here. In section 3, we show a clear correlation of the total radiated power (P_{rad}) with the APL W source intensity during start-up. In section 4, we investigate the effect of B and N impurities on APL W sputtering. Finally,

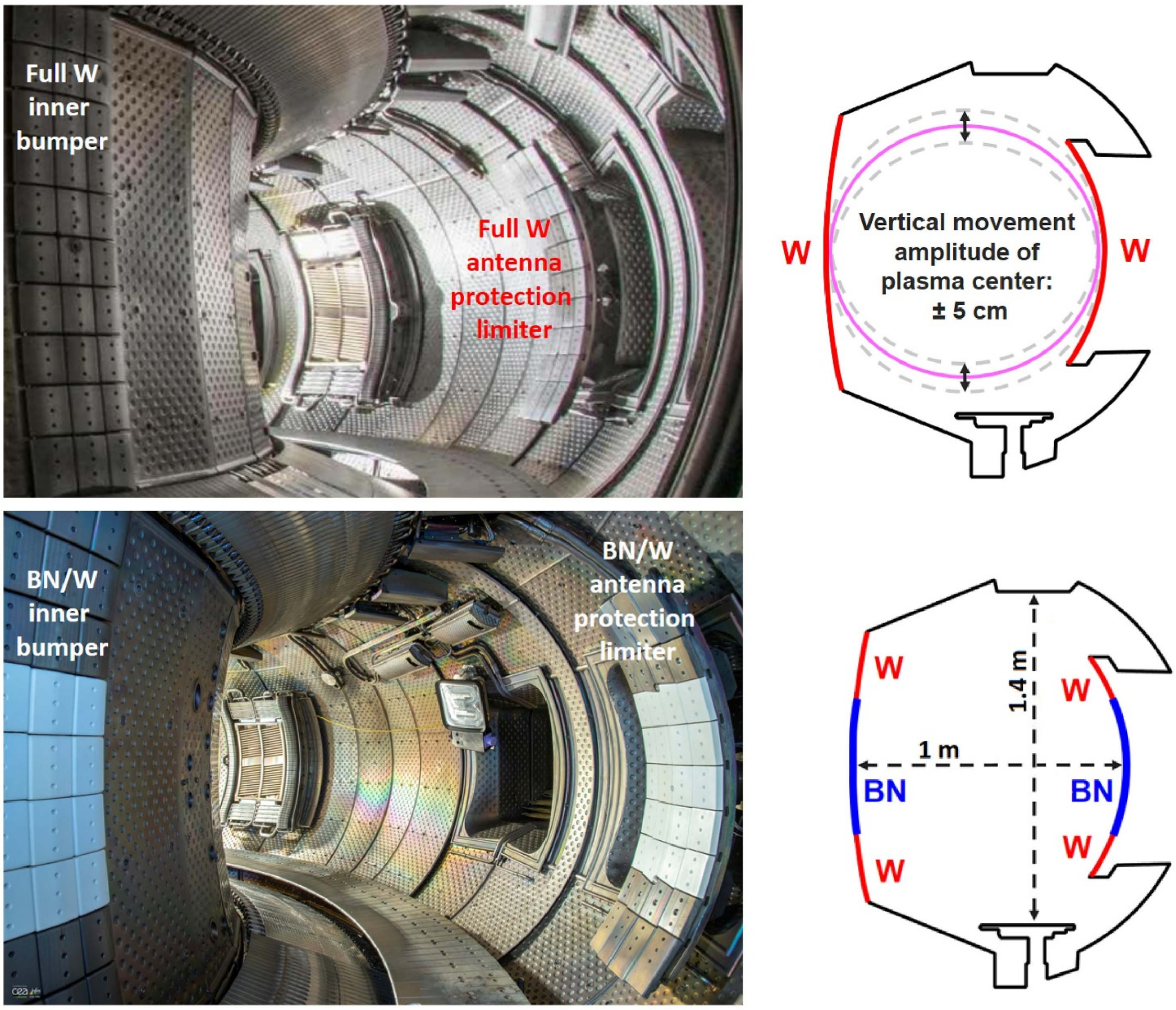

Figure 1. Top: WEST plasma chamber with full W first wall (left) and the average vertical amplitude of plasma movement (right). Bottom: WEST plasma chamber with BN/W first wall (left) and the dimensions of the chamber (right).

in section 5, we analyze the legacy effect of B powder drops on start-up conditions in a number of discharges in the 2020 and 2023 campaigns. We conclude on the effect of these different actuators on WEST start-up conditions in the context of ITER and future fusion power plants.

2. Experimental conditions

In figure 2, we can see 3 examples of start-up phases in WEST in 2019, 2020 and 2023 campaigns with respectively full W and then BN/W first wall elements. During these campaigns, according to NICE magnetic equilibrium reconstructions [11], a typical plasma start-up on WEST involves a contact with the APL ∼100 ms after breakdown. The plasma then moves towards the IB where it stays until X-point creation, which can happen as soon as ∼700 ms. At this moment, the APL, meant to protect the antennas against possible runaway electrons during the start-up phase, is retracted for divertor operations.

We can see in figure 2 that for similar start-up dynamics in terms of plasma position, current ramps, pre-magnetization and gas prefill, the amount of power radiated and the intensity of the WI emission on the IB and the APL can vary significantly depending on the wall material. In any case, a transient increase of the WI emission and $P_{\rm rad}$ occur at the same time on the APL, while the correlation between the IB W source and $P_{\rm rad}$ is less evident. With full W first wall elements, the level of radiation is higher by a factor ∼2 and the WI intensities are ∼1-2 orders of magnitude higher than with the 2020 BN/W first wall. Interestingly, for the 2023 campaign with the same BN/W first wall as in 2020, it can be noticed that the level of radiated power and WI emission are similar or higher than with a full W first wall. This will be discussed in more details in the next sections.

In order to compare the effect of boronizations on plasma start-up with full W first wall (2019 campaign) and BN/W first wall (2020 and 2023 campaigns), we have selected series of discharges following boronizations performed with an equivalent amount of boron (∼10 g each time), see table 1. All the analysis presented here are focused on the start-up phase and were performed during the first 500 ms of plasma in order to have comparable configurations with the APL at the same position.

On WEST, the impurity sources on the IB and the APL are observed by the visible spectroscopy system [12]. The IB is in sight of a single telescope sending the visible light to a 600 mm^{-1} grating spectrometer through several meters of optical fiber bundles. This spectrometer covers the domain of wavelength between 385 nm and 445 nm. The APL is observed by two telescopes, which send the visible light to a similar 600 mm^{-1} grating spectrometer. In the 2019 campaign, the wavelength between 360 nm and 420 nm were covered and in the 2020 and 2023 campaigns, this domain was shifted to 385–445 nm. For both systems, the lines of sight (LOS) available (figure 3) were used to calculate a total amount of photons collected over the IB and the APL for the first 500 ms of plasma.

The power radiated by the plasma and measured by the bolometers is a valuable information here since it is often related to the presence of impurities. In particular, it is a good indicator for the presence of W in the plasma core [6]. In the

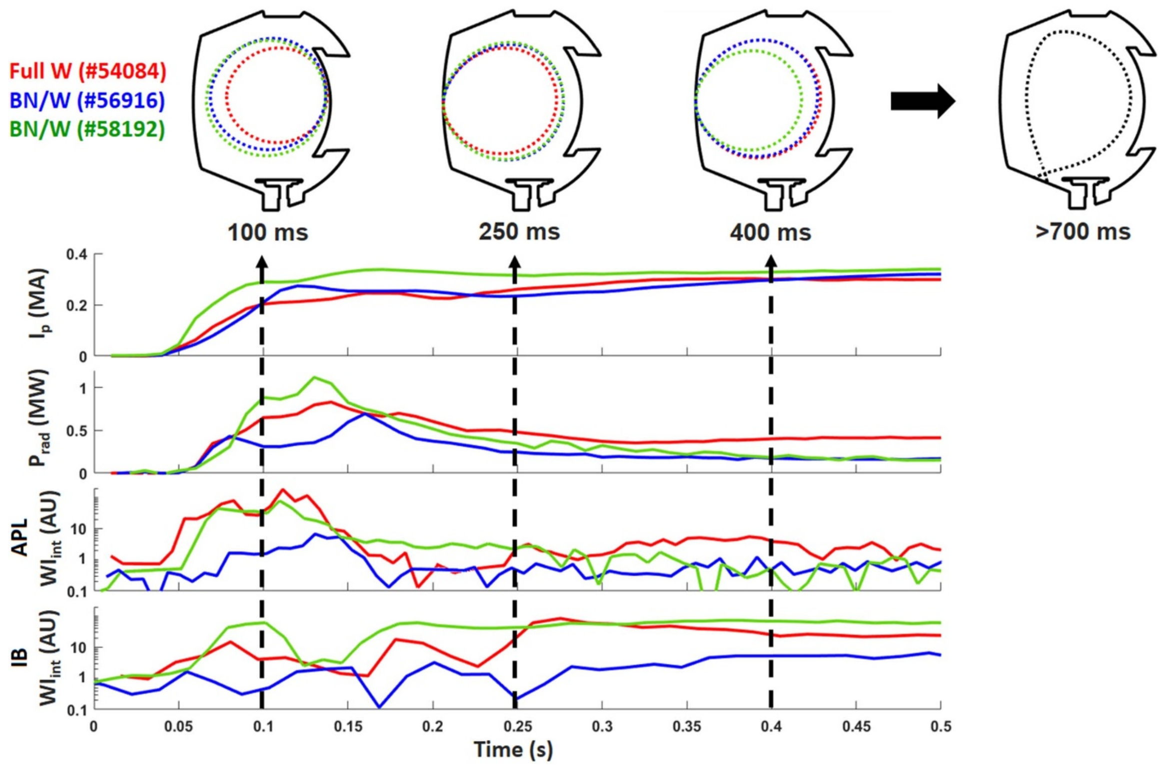

Figure 2. Evolution of the magnetic equilibrium with the time-traces for the plasma current ($I_{\rm p}$), the $P_{\rm rad}$, the APL and IB WI intensity signals during start-up for the 500 ms time window used for this study.

Table 1. Series of discharges used.

Campaign	2019 campaign (Full W)		2020 campaign (BN/W)		2023 campaign (BN/W)	
Shot series	#55000–#55136	#55137–#55242	#56244–#56594	#56595–#56927	#57171–#57839	#57840–#58687

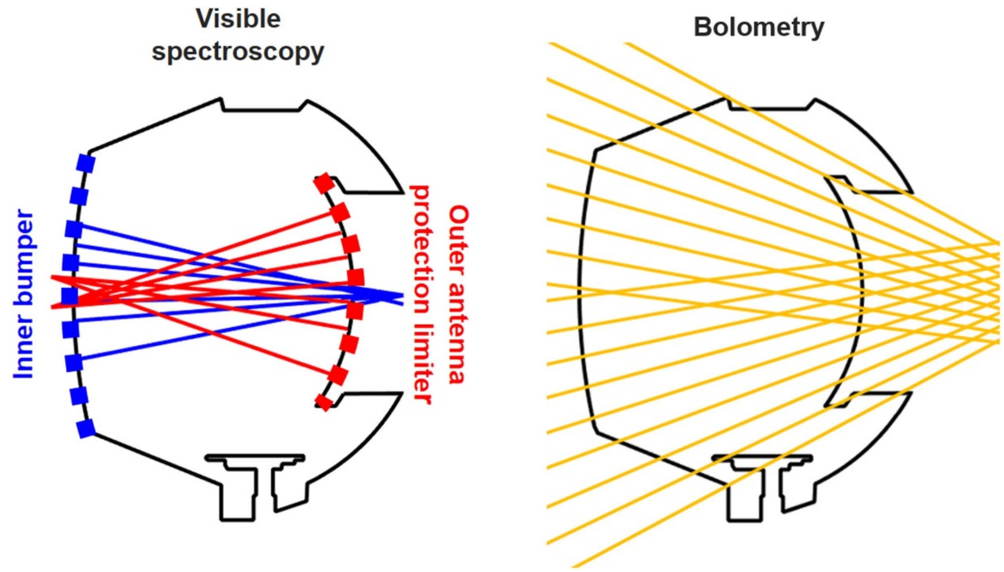

Figure 3. Left: visible spectroscopy LOS used for this plasma start-up study. Right: bolometry LOS used for the calculation of the start-up $<P_{\mathrm{rad}}>$.

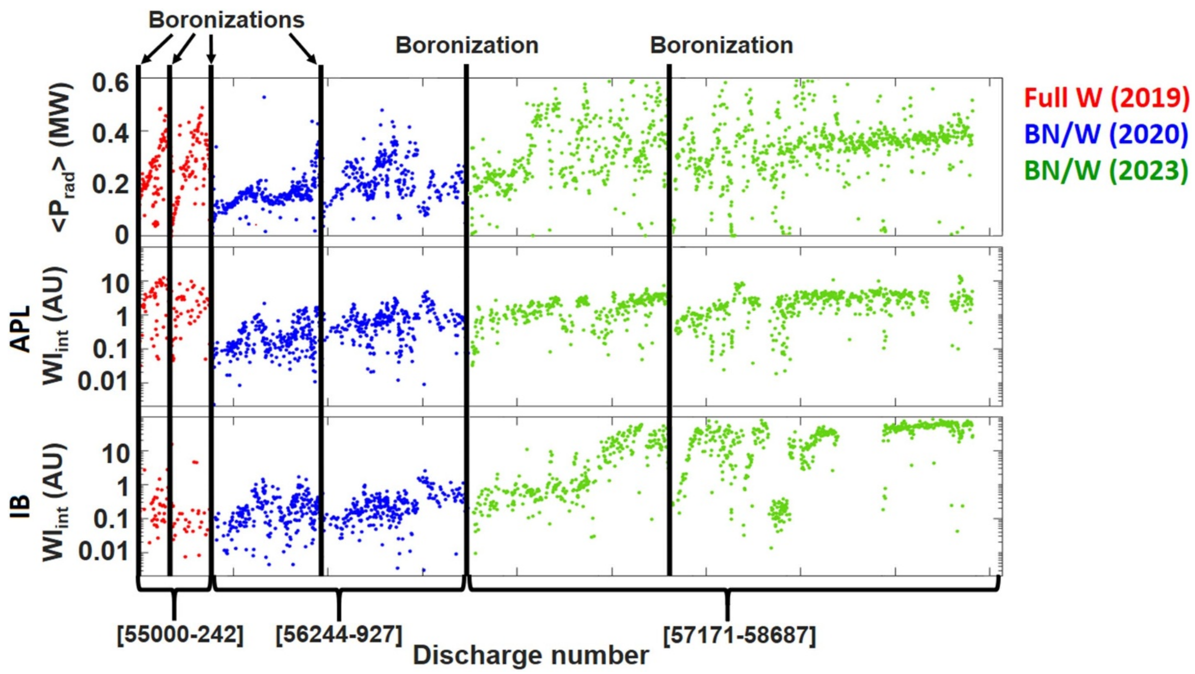

Figure 4. $<P_{\mathrm{rad}}>$ and integrated APL and IB WI intensity database for the series of start-up discharges selected here.

present work, we are looking for actuators to minimize the core radiation during start-up. In all the discharges considered here, the total P_{rad} is produced by integration over the available bolometry LOS [13] (figure 3) and is averaged over the first 500 ms of plasma to produce $<P_{\mathrm{rad}}>$.

This bolometry and spectroscopy data was used for all the discharges selected in table 1 to create a database of $<P_{\mathrm{rad}}>$ and WI (at 400.9 nm), BII (at 419.5 nm), NII (at 399.5 nm) and DI (at 410.1 nm) time-integrated intensities over the IB and the APL. Figure 4 shows the evolution of some of this data with the selected discharge numbers. For each discharge, the total deposited energy on the limiters during the early plasma phase and the termination is around ∼1 MJ.

It can be noticed by looking at figure 4 that boronizations strongly reduces $<P_{rad}>$ and that the changeover from W tiles to BN tiles on the first wall initially reduced the APL WI intensity by ∼2 orders of magnitude. We can also observe a gradual increase of this WI signal over the 2020 and 2023 campaigns to reach an intensity comparable to what was measured with the full W first wall at the end of the 2019 campaign. This will be commented in the next Section below.

3. Radiated power and first wall W sources during plasma start-up

We have investigated possible relations between $<P_{rad}>$ and the intensity of W sources sputtered by light impurities like B, N, oxygen (O) or carbon (C) from the IB and the APL in the selected start-ups of table 1. On figure 5, we can see a clear non-linear increase of $<P_{rad}>$ with the WI line time-integrated intensities over the APL for all campaigns. On the other hand, it seems that there is no obvious relation between $<P_{rad}>$ and the IB time-integrated WI line intensity. This strong in/out asymmetry in terms of contribution to plasma core radiation could be linked to low field side turbulence ballooning [14] which allows the inward transport of impurities like W. On the high field side, the laminar nature of SOL flows would screen the plasma from the inboard first wall W impurity source.

We can also notice that the changeover from full W first wall to BN/W for the 2020 campaign comes with a reduction of $<P_{rad}>$ by ∼30% and a strong drop of the integrated WI line intensity by an order of magnitude on both the IB and the APL. However, for the 2023 campaign with the same BN/W first wall, we can clearly see that $<P_{rad}>$ and the IB and APL integrated WI intensities are closer or higher than what was measured in 2019 with the full W first wall.

The strong increase of WI emission on the BN/W first wall in the 2023 campaign suggests significant W migration and accumulation on the BN surfaces. The presence of a W deposit is also confirmed by post-mortem analysis of the BN tiles by x-ray fluorescence spectroscopy. The W enrichment process on BN tiles with light B and N atoms being sputtered more easily than heavy W atoms is likely to be responsible for the accumulation of the latter. Interestingly, a similar phenomenon was already observed in 1982 in ASDEX with iron migrating from stainless steel plasma facing elements and accumulating as deposits on C limiters [15].

In WEST, the W deposited on the IB (see figure 6) and APL BN tiles may have multiple origins. For example, during the X-point phase, the divertor W source is strong and lasts from tens to hundreds of seconds but the plasma should screen the IB and the APL from it.

The migration of the W from the edges of the IB and the APL made of W tiles may also be a possibility but the duration of their contact with the plasma is only of the order of a ∼1 s per pulse. More work is needed on this topic to conclude on the dominant contributor.

In any case, keeping the plasma on the IB during start-ups like in ASDEX-Upgrade [16] seems to be a solution for a reliable and stable initial phase with a full W first wall in WEST.

4. Effect of B from boronizations and N injections on outer wall W sources

Boronizations performed in dedicated glow discharges in WEST [17] cover all surfaces with a thin layer of B which transiently replaces detrimental W sputtering by harmless B sputtering. B is also a good getter of O and the trapping of the latter on recessed surfaces leads to continued reduced W sputtering when the boron layers are eroded away on plasma-wetted surfaces. B being a low Z, poorly radiating impurity [18], is expected to improve plasma conditions while it is eroded. We have studied its effect on start-up plasmas here for the series of discharges of table 1 for the 2019, 2020 and 2023 campaigns.

Given the prominent role of the APL W source on the start-up radiated power in WEST, figure 7 focuses on the comparison of WI/DI to BII/DI line intensity ratios over this object. Line ratios are used to remove the dependence on electron temperature and density of the line intensities, which are similar for WI, BII and DI. The color of the dots gives information on the associated $<P_{rad}>$. Only cases without N injection are considered here in order to isolate the effect of B only. Therefore, figure 7 gives information on the relation between the concentration of W and the concentration of B in the plasma on the APL surface during start-up. Right after boronization, the BII/DI ratio is expected to rise significantly and to progressively decrease while B leaves the first wall surfaces to accumulate in less exposed areas.

In figure 7, the small number of points for the 2019 campaign is due to the limitation of the database to the series of discharges using D (several sessions used helium) and following boronizations performed with the same amount of B. Despite this reduced number of cases, a trend can still be observed with a decrease of the WI/DI ratio by ∼2 orders of magnitude as well as a significant drop of $<P_{rad}>$ with the increase of the BII/DI ratio. In the 2020 campaign, a number of plasmas seem to benefit from boronizations but the trend is not as clear as in 2019. The situation degrades even further in the 2023 campaign, with the WI/DI ratio and $<P_{rad}>$ increasing with the BII/DI ratio. It is possible that the W deposit covering the BN surfaces does not have good binding properties with the material below as well as with a B layer on top. In this case, it may be sputtered more easily even after a boronization. This would require further investigations based on post-mortem analysis of the BN tiles. In the three campaigns, we can clearly see that $<P_{rad}>$ depends strongly on the WI/DI ratio on the APL, consistently with figure 5 above.

We have also studied the impact of N from injections during start-up [7], from radiative divertor experiments legacy or sputtered from the BN tiles. When N is seeded during start-up, the valve is opened from the breakdown to a few seconds after.

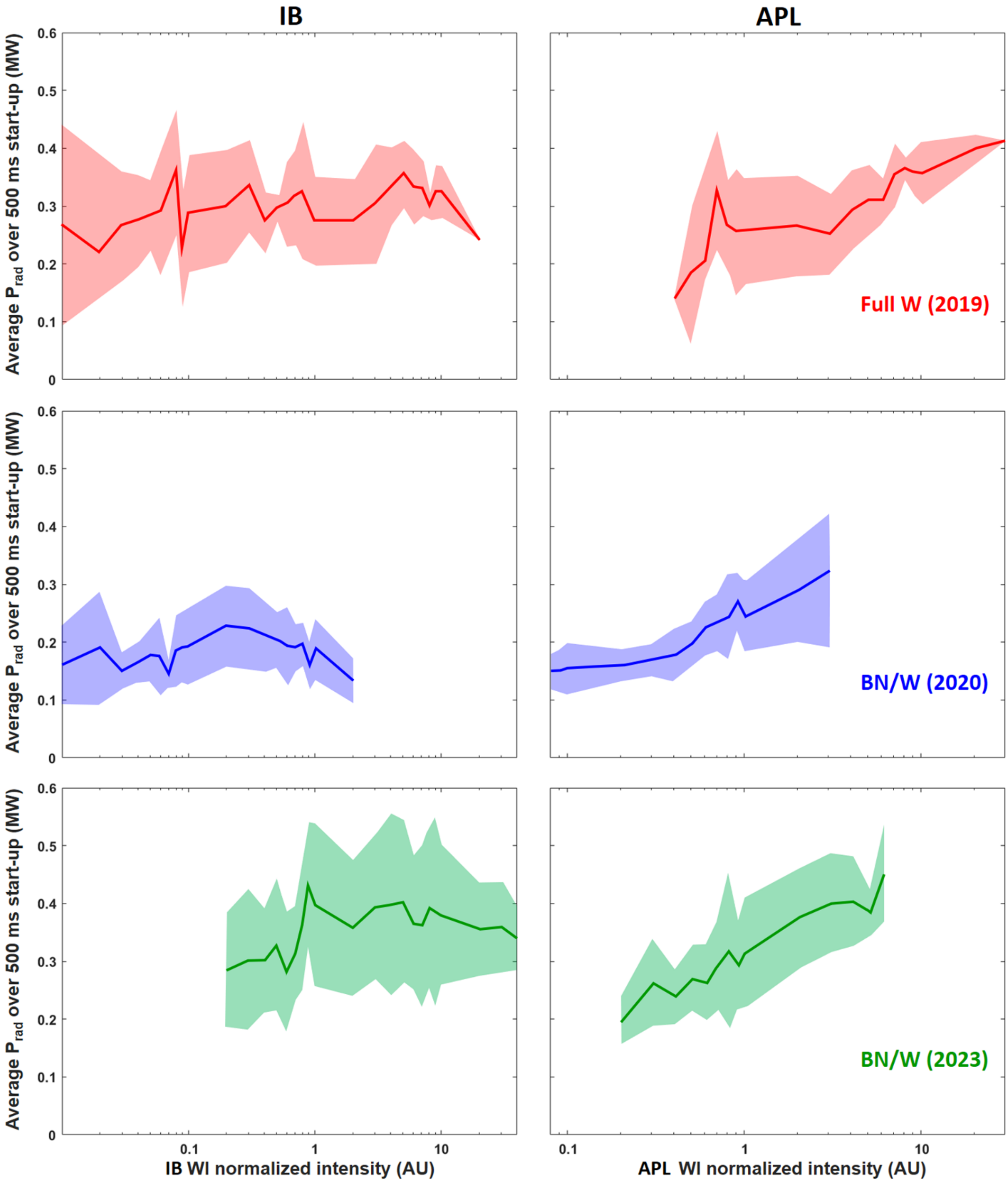

Figure 5. Evolution of $<P_{rad}>$ with integrated WI line intensity (log scale) on the IB and the APL with a full W first wall (2019) and a BN/W first wall (2020 and 2023).

In figure 8, we compare the WI/DI ratio to the NII/DI ratio on the APL during plasma start-up in the 2019, 2020 and 2023 campaigns. Here, the ∼50 discharges following boronizations were not accounted for in order to characterize in the best possible way the effect of N alone.

We notice in figure 8 that for the 2019 campaign, the presence of N on the first wall during start-up, measured by the increase of the ratio NII/DI, produces very sparse results ranging from nearly no reduction to more than ∼2 orders of magnitude reduction of the WI/DI ratio. The reason for this is unclear at this stage. The return to a full W first wall at the end of 2024 will allow more studies on this topic. For the 2020 and the 2023 campaigns, N injection seems more clearly beneficial with a reduction of the WI/DI ratio by up to ∼2 orders of magnitude.

For the $<P_{rad}>$, we can notice a similar dependence with the WI/DI ratio as in figure 7. Surprisingly, although N is known to be a good SOL radiator [18], we can see that for the few cases with the highest NII/DI ratio and the lowest WI/DI ratio, in the 2020 and the 2023 campaigns, $<P_{rad}>$ can be significantly reduced. The radiative cooling of N during start-up may be just sufficient to reduce the impact energy

Figure 6. Example of IB surfaces with BN tiles after installation in 2020 and before removal in 2024.

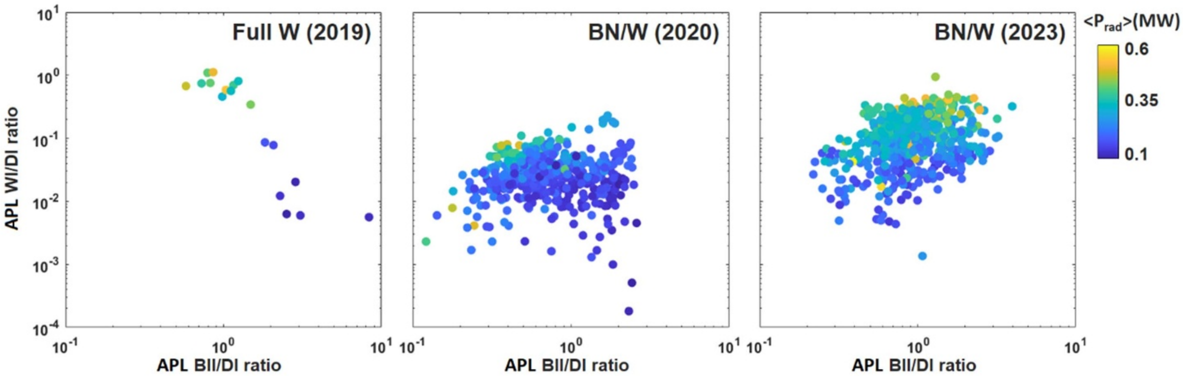

Figure 7. Evolution of the start-up WI/DI ratio with the BII/DI ratio on the APL in the 2019, 2020 and 2023 campaigns. The color of the dots gives information on the level of $<P_{\mathrm{rad}}>$ in each case.

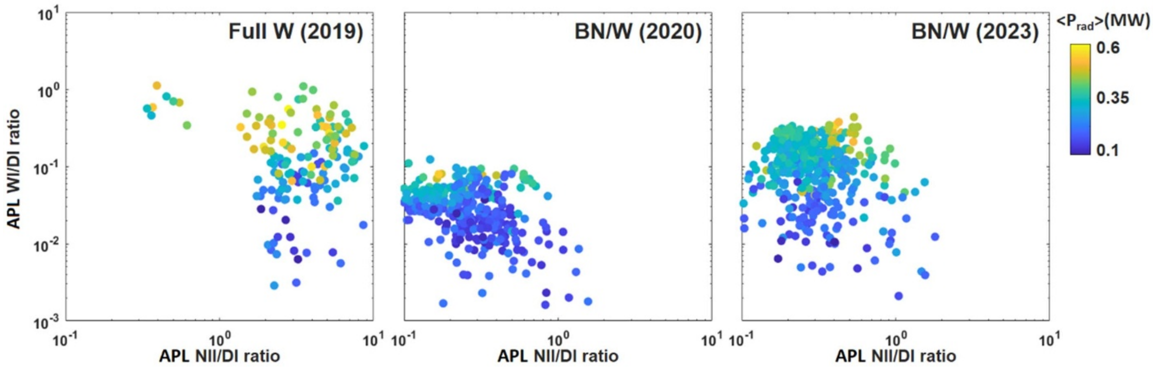

Figure 8. As figure 7 for the evolution of the WI/DI ratio with the NII/DI ratio on the APL.

of light impurities like B, N, C or O below the W sputtering threshold. Interestingly, the level of SOL radiation needed for this observed W sources reduction turns out to be significantly smaller than the level of W core radiation when the W sources are strong. However, for many cases in the 2019 campaign and also the intermediate values of NII/DI ratios in 2020 and 2023, N seeding during start-up is associated with high levels of $<P_{\mathrm{rad}}>$.

Overall, the presence of N impurities during start-up can have similar benefits as boronizations in terms of W sources and $<P_{\mathrm{rad}}>$ reduction during start-up without accumulating in the machine. In addition, N has some other advantages over

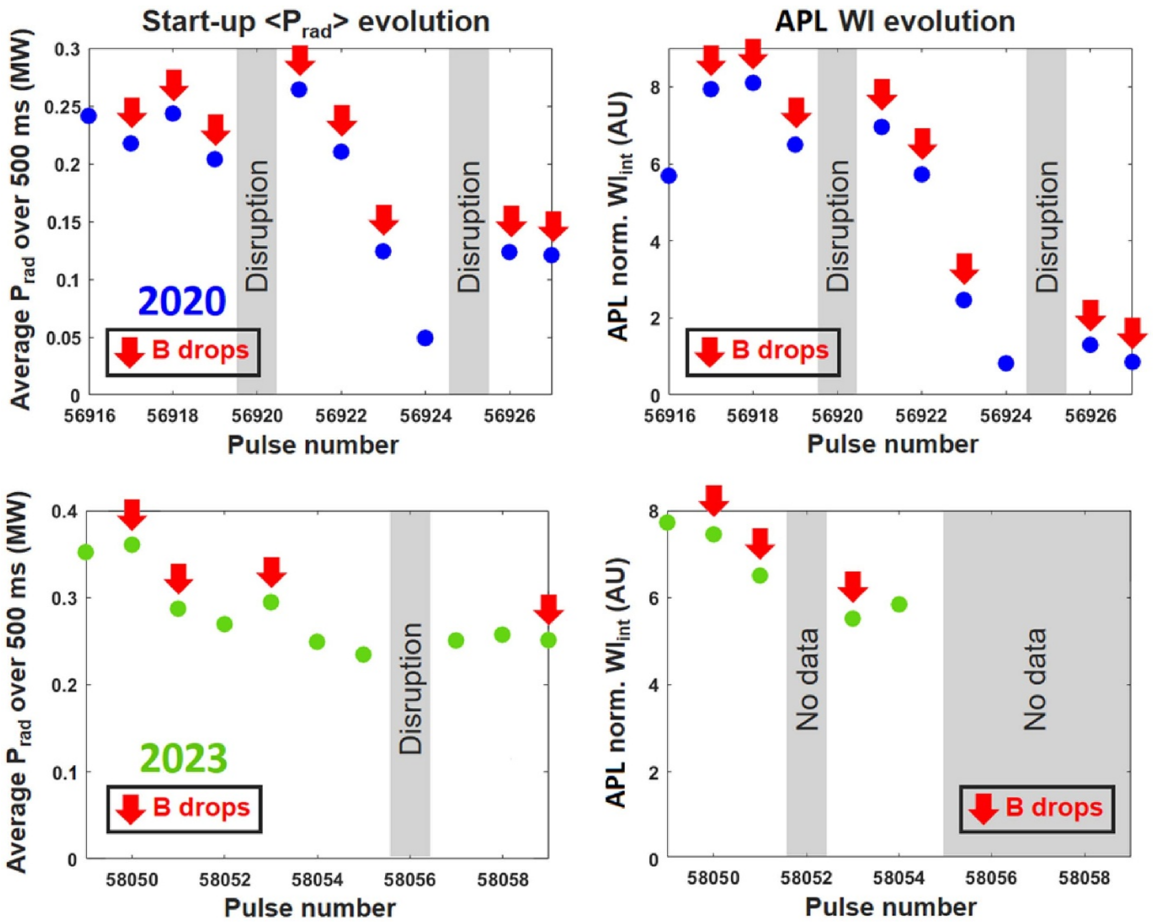

Figure 9. Top: evolution of $<P_{\text{rad}}>$ (left plot) and APL WI brightness (right plot) for the discharges with B powder drops in the 2020 campaign. The red arrows show in which discharge the B drops occurred. Bottom: same as the top but for the 2023 B powder drops session.

boronizations: N is easy to inject and pump out while boronizations require long dedicated glow discharges with the handling of B_2D_6, which is very toxic. Although, the accumulation of B in the tokamak on surfaces less exposed to the plasma keeps helping with O gettering, B itself contributes to W sputtering once the latter is uncovered, which leads to the need for more boronizations. This is evidenced in figure 7 where a good number of discharges in 2020 and 2023 campaigns with high BII/DI ratios are essentially associated with high WI/DI ratios. Moreover, in a deuterium/tritium machine, the trapping of tritium with the accumulated B would also be a problem.

5. Impact of B from powder drops on plasma start-up conditions

For an easier approach to wall conditioning with B and performance improvements, WEST was equipped for the 2020 campaign with the Princeton Plasma Physics Laboratory impurity powder dropper [8, 10], a system capable of dropping impurity powder in real time during plasma discharges. B powder drops were performed during one session in the 2020 campaign [8] and for another session in the 2023 campaign [9, 10]. Here we have used these tests to look at the effect of B powder drops on the start-up plasma of the next discharge.

In figure 9, we show the evolution of the start-up $<P_{\text{rad}}>$ and APL WI brightness for each discharge (approximately ∼1 MJ of deposited energy on the limiters) following a drop of B powder in the 2020 campaign (blue dots). As in the previous section, we focus on the APL here because of the strong correlation between its W source and the plasma start-up $<P_{\text{rad}}>$. From discharge #56921, where the cumulated amount of B powder dropped went beyond 100 mg [8], we can see a clear fall of $<P_{\text{rad}}>$ and WI intensity by more than 80% after only three discharges with B powder drops. The experiment was then perturbed by a disruption but we can see low $<P_{\text{rad}}>$ and APL WI brightness start-up conditions for the last two discharges. In total, ∼0.3 g of B powder were used over this session.

In figure 9, we can also observe the effect of B powder drops in the 2023 session (green dots) with a reduction of $<P_{\text{rad}}>$ and APL WI intensity after each B powder drops. However, the effect is significantly weaker since both signals are decreased by less than 30% despite ∼0.9 g of B dropped in total over four discharges.

The accumulation of W observed on the BN tiles in the 2023 campaign could explain why B powder drops are less effective. Indeed, they are expected to act like small-scale boronizations [8] with the creation of a thin B layer on W surfaces. In the 2020 campaign with the new BN tiles, little

B powder was needed to cover the small first wall W sources observed in figure 5. In 2023, the B powder drops may have not been sufficient to cover the significantly larger W source from the deposit covering the same BN tiles. This would suggest that B powder drops may be less effective than boronization or N seeding at reducing $<P_{rad}>$ and W sources on pure W limiters in WEST.

In fact, it was actually shown in two B powder drops dedicated session in ASDEX-Upgrade [19] with similar total amounts injected (∼0.3 and ∼1 g) that WI emission noticeably increases with the BII emission on the outboard antenna limiter. It seems that in the full W environment of ASDEX-Upgrade, B from powder drops does not have a protective role on W surfaces in this region but is rather responsible for W sputtering. Further investigations will be carried out on this topic on WEST in the late 2024 campaign with the return to a full W first wall and dedicated B powder drop experiments.

6. Conclusions

Series of start-up plasmas achieved with a high Z (full W limiter tiles) and low Z (BN central limiter tiles) first wall with similar boronization conditions were studied in WEST in the context of the ITER first wall being covered with tungsten (W) instead of beryllium [20]. According to the results from WEST presented here, the total radiated power during start-up is strongly correlated with the WI/DI emission on the outer movable limiter. Start-ups on the inner wall like in ASDEX-Upgrade [16] help stabilizing the plasma with a high Z first wall. This could be related to the better screening from impurities in this region due to the laminar nature of the high field side SOL transport. This should be investigated in future work.

The effect of boron (B) from different sources on plasma start-up conditions was also investigated:

- B from low Z (BN) tiles: WI spectroscopy shows that they are progressively covered with a W deposit probably by migration and enrichment by preferential sputtering of the lighter B and nitrogen (N) elements. The migrating W may originate from the remaining W first wall elements during start-up or the divertor monoblocks during X-point operations but it is not yet clear which contribution dominates.
- B from boronizations: they can reduce the first wall W sources but their impact is short living because of the quick removal of the B layer covering the W surfaces [17].
- B from powder drops: they act like small-scale boronizations [8–10] but their benefit on first wall W sources and $<P_{rad}>$ reduction tends to weaken with the accumulation of W deposits on the BN tiles. This result suggests that it may be less effective with a high Z first wall. The late 2024 WEST campaign with a full W first wall will tell us if it could be an interesting solution for ITER plasma start-ups.

In any case, B tends to accumulate in the machine and contributes to W sputtering in the end. On the other hand, N injections during start-up [7] can be as efficient as B in terms of first wall W sputtering and $<P_{rad}>$ reduction but without accumulating. Since in ITER, Ne will be preferred to N, one can wonder if such a strong radiator can be introduced as early as during plasma start-up.

On ITER, the use of electron cyclotron heating during this phase should allow surviving high W concentrations in the core as already shown in ASDEX-Upgrade [16] but will increase the impurity ions impact energy and therefore W sputtering. An optimized use of B and Ne during powered start-ups is to be investigated in the context of the new ITER baseline [20–22]. This will be the object of future work in the next WEST campaigns with a full high Z first wall and electron cyclotron heating [23].

Acknowledgment

This work has been carried out within the framework of the EUROfusion Consortium funded by the European Union via the Euratom Research and Training Programme (Grant Agreement No. 101052200). The views and opinions expressed are however those of the authors only and do not necessarily reflect those of the European Union or the European Commission. Neither the European Union nor the European Commission can be held responsible for them.

ORCID iDs

K. Afonin https://orcid.org/0000-0002-5479-2897
G. Bodner https://orcid.org/0000-0003-2497-9172
Y. Corre https://orcid.org/0000-0002-6566-6116
P. Devynck https://orcid.org/0000-0001-6752-9345
A. Diallo https://orcid.org/0000-0002-0706-060X
A. Gallo https://orcid.org/0000-0002-7472-7830
R. Lunsford https://orcid.org/0000-0003-3588-6801
P. Maget https://orcid.org/0000-0002-8746-8102
J. Morales https://orcid.org/0000-0002-3140-0504

References

[1] Bucalossi J. *et al* 2022 *Nucl. Fusion* **62** 042007
[2] Bourdelle C. *et al* 2015 *Nucl. Fusion* **55** 063017
[3] Gunn J.P. *et al* 2021 *Nucl. Mater. Energy* **27** 100920
[4] Firdaouss M. *et al* 2017 *Fusion Eng. Des.* **124** 207–10
[5] Tsitrone E. *et al Nucl. Mater. Energy* submitted
[6] Ostuni V. *et al* 2022 *Nucl. Fusion* **62** 106034
[7] Maget P. *et al* 2022 *Plasma Phys. Control. Fusion* **64** 045016
[8] Bodner G. *et al* 2022 *Nucl. Fusion* **62** 086020
[9] Afonin K. *et al* 2024 *Nucl. Mater. Energy* **40** 101724
[10] Lunsford R. *et al* 2024 *Nucl. Mater. Energy* **40** 101726
[11] Faugeras B. *et al* 2020 *Fusion Eng. Des.* **160** 112020
[12] Meyer O., Giacalone J.C., Gouin A., Pascal J.Y., Klepper C.C., Fedorczak N., Lotte P., Unterberg E.A., Fehling D.T. and Harris J.H. 2018 *Rev. Sci. Instrum.* **89** 10D105
[13] Devynck P., Fedorczak N., Mao R. and Vartanian S. 2021 *J. Phys. Commun.* **5** 095008
[14] Fedorczak N., Gunn J.P., Ghendrih P., Ciraolo G., Bufferand H., Isoardi L., Tamain P. and Monier-Garbet P. 2011 *J. Nucl. Mater.* **415** S467–S70
[15] Hengelhardt W. *et al* 1982 *J. Nucl. Mater.* **111 & 112** 337–42
[16] Fietz S., Fable E., Hobirk J., Fischer R., Fuchs C., Pereverzev G. and Ryter F. 2013 *Nucl. Fusion* **53** 053004
[17] Gallo A. *et al* 2024 *Nucl. Mater. Energy* **41** 101741

[18] Summers H.P. 2004 Atomic data and analysis structure user manual 2nd edn (available at: www.adas.ac.uk)
[19] Krieger K., Balden M., Bortolon A., Dux R., Griener M., Hegele K., Laggner F., Rohde V. and Wampler W.R. 2023 *Nucl. Mater. Energy* **34** 10137
[20] Loarte A. *et al* Initial evaluations in support of the new ITER baseline and Research Plan (available at: https://www.iter.org/sites/default/files/media/2024-04/itr-24-004-baseline-ok.pdf)
[21] de Vries P.C. *et al* 2013 *Nucl. Fusion* **53** 053003
[22] Kim H.-T., Fundamenski W. and Sips A.C.C. 2012 *Nucl. Fusion* **52** 103016
[23] Delpech L. *et al* 2023 *Fusion Eng. Des.* **186** 113360